Sensors & Transducers
Published by IFSA Publishing, S. L., 2017
http://www.sensorsportal.com

Review on Ultra-Sensitive QCM Mass Sensor and Microfluidic for Diagnostic Point of Care

Selemani SEIF, Thomas THUNDERT and * Kenneth CADIEN
University of Alberta, Department of Chemical & Materials Engineering
9211-116 Street NW, Edmonton, Alberta, Canada T6G 1H9
* Tel.: (780) 492 7380
* E-mail: kcadien@ualberta.ca

Received: 14 July 2017 /Accepted: 15 August 2017 /Published: 31 August 2017

Abstract: This review discusses on Quartz Crystal Microbalance (QCM) and microfluidic driven by ultrasonic acoustic forces, as possible alternative technologies to develop compact and portable diagnostic point of care (POC). Extension of QCM to measure 10^{-15} g/cm^2 is possible and development of this technology will open up new business opportunities in public health, life sciences, and material sciences. The experimental results showed that QCM technology can be 1000 times more sensitive, than the currently available mass sensor systems in the market. The target market is on diagnostic POC, focussing on home care, public health, and agriculture and food industry sectors. Some of the challenges discussed are: 1) A centrifuge for blood plasma separation (BPS), and 2) Microfluidic driven by ultrasonic acoustic forces, for separation of suspended particles in the whole blood. We also present an overview of the expected global market growth from 2011 to 2020 and the benefits to the end users.

Keywords: Femtogram, QCM, Microfluidic, Ultrasonic blood plasma separation (BPS), Free-BPS, Whole blood.

1. Introduction

The CANARY/PANTHER technology is currently used as diagnostic POC for detection of virus and bacteria in site buildings, emergency response, and rapid screening of other disease outbreak in public areas, but encounters a lot of problems. These problems are primarily sample preparation [1-2], involving micro-centrifuges, and micro-air handling devices, burdened by the long-term storage of refrigerated B-cells, which are ineffective in other applications. Mass Spectroscopy (MS) and electron microscopy are very effective in conducting scientific research and can be used for identification of diseases in several hours or weeks, but face challenges such as miniaturization, preprocessing samples, introducing samples to the MS chamber, and interpreting spectral signals. Therefore, there is a need to develop cost-effective portable diagnostic POC equipment for detection of diseases in real time.

The nanoscale mass sensor devices which can be used to develop cost-effective and modern diagnostic POC systems do exist and the patents have been reported elsewhere [3-14]. The existing inventions are sensitive enough to measure the mass of bacteria, virus, cells, molecules, and troponins. These devices are based on Carbon Nanotube (CBN), QCM, Micro-Electromechanical Systems (MEMS), and Microcantilevers, with the capability to measure mass from picogram (pg/cm^2 or 10^{-12} g/cm^2) to zeptograms (zg/cm^2 or 10^{-21} g/cm^2). Among these devices, the only one which is cost-effective, cheap, easy to fabricate and manufacture, and commercially available in the market, is QCM mass sensors [15-18].

Sauerbrey [19] was the first to recognize the potential usefulness of the QCM technology and demonstrated the mass sensitivity nature towards frequency changes at the surface of QCM electrodes. He derived the equation which relates the mass change per unit area at the QCM electrode surface to the observed change in oscillation frequency of the crystal as shown in the expression: $K = 2f^2/\sqrt{\rho\mu} = 2.26\times10^{-6} f^2 Hz^{-1} cm^2/g$, where K is the mass sensitivity coefficient, ρ = 2.648 g/cm^3, is the density of quartz crystal, and $\mu = 2.947\times10^{11}$ g/cm.s^2, is the shear modulus of quartz crystal. If the mass sensitivity coefficient (K) and the detection limit Δf (τ) parameters are known, it is possible to estimate mass resolution; using Allan deviation σ (τ) which represents noise instability in the time domain less than 10 seconds [20-21]. The σ (τ) is calculated using the equation; $\sigma = (1\times10^{-7})/Q$, where Q is the Q-factor of an AT-cut quartz disk. The Δf (τ) is calculated using the equation; $\sigma (\tau) \times f (\tau) = \Delta f (\tau)$, while the mass resolution [22] is calculated by taking the ratio of Δf (τ) to K.

To verify that the mass resolution depends not only on the frequency shift but also the diameter of the central active electrode, we have designed, fabricated, and characterized 5 disks. The diagrams which show the designs and the experimental set-up for measurement of the Q-factors and the frequencies are shown in Sections 3 and 4. Section 5 discusses on calculated σ (τ), K, Δf (τ), and mass resolution in g/cm^2. Sections 6 and 7 discuss on challenges for developing diagnostic POC using QCM mass sensor interfaced with microfluidic driven by ultrasonic acoustic forces. Section 8 discusses on market overview and benefits to end users while the last section summarizes what has been discussed in this review.

2. Design, Fabrication and Characterization of the Disks

The disks were designed and fabricated using sputter deposited Gold electrode layers (~300 nm) on Chromium adhesion layer (~50 nm). The diagram which shows the fabricated disks is depicted in Fig. 1.

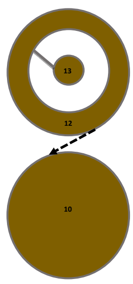

Fig. 1. The top views show the gap with numeral 11, the ring electrode with numeral 12, and the center electrode with numeral 13. The bottom side is a full coated electrode with numeral 10.

Referring to Fig. 1, the top side of the disk is described using three numerals; 11, 13 and 12. Numeral 11 is the gap between the center electrode and the outer ring electrode. Numeral 13 is the center electrode as viewed from the top of the Quartz disk. Numeral 12 is the ring electrode, at the bottom side of the Quartz disk, is the full electrode marked with numeral 10. The center dot with numeral 13 has different diameters (1 mm, 2 mm, 3 mm, 4 mm and 5 mm) for disks 1 to 5 respectively.

3. Experimental Set-up

The experimental set up for Q-factor measurements using 4294A Precision Impedance Analyzer which is connected to Signatone (S-1160 model) Probe Station is shown in Fig. 2 (a).

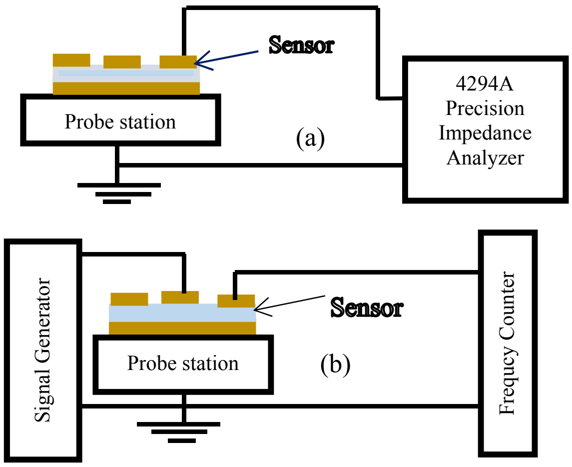

Fig. 2. (a) Set-up for measurements of Q-factors versus frequencies; (b) Set-up for measurement of frequency stability.

These disks were mounted on a Signatone (S-1160 model) Probe Station and connected using a coaxial cable to the 4294A Precision Impedance Analyzer in the series configuration. The electrical signal (150 mV) is applied at a resonant frequency on the top layer labeled with numeral 12 while the ground terminal is connected to a full bottom electrode labeled as numeral 10. The measured parameters were Q-factors, in the frequency range between 1 MHz and 1.10 MHz The set-up for frequency shift measurements using Frequency Counter, Signal Generator, and Signatone (S-1160 model) Probe Station is shown in Fig. 2 (b). The disks were mounted on the top of the probe stations and the sinusoidal electrical signals (10 V) were applied from the signal generator to the ring electrode while the full bottom electrode grounded. The Frequency Counter was then used to measure frequencies using lab view program installed in the computer.

4. Results and Discussion

In this section we present results based on:

1) Q-factors and Allan deviation calculation;
2) Calculation of mass sensitivity coefficients;
3) Calculation of detection limit;
4) Calculation of mass resolution.

4.1. Q-factors and Allan Deviation Measurements

The curve which shows the measured Q-factors versus frequencies is in Fig. 3(a), the obtained results show the maximum Q-factor to be 50000 at resonance (1.067 MHz) for the disk with 3 mm diameter. For the disks with 1 mm, 2 mm, 4 mm and 5 mm, diameters, the measured Q-factors were 40000, 46000, 42000 and 38000 respectively.

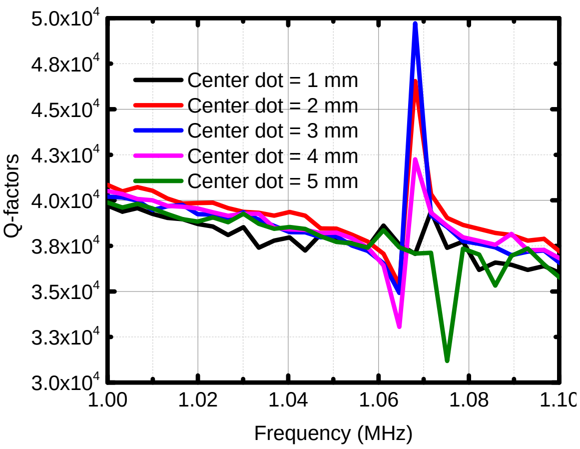

Fig. 3 (a). The curve which shows the measured Q-factors of five disks as a function of frequencies and the diameters of the central electrodes.

The curve which shows the calculated Allan deviation is in Fig. 3 (b). The highest Allan deviations were calculated from the disks with 5 mm and 4 mm diameters; the σ (τ) of the disk with 5 mm as a central diameter was 3.2exp-12, while the σ (τ) of the disk with 4 mm as a central diameter was 3.05exp-12. The disk with the smallest Allan deviation was that with 1 mm diameter, where σ (τ) is equal to 2.7ex-12. By comparing the results obtained in Fig. 3 (a) and (b) we noted that as Q-factors increases the value of calculated σ (τ) decreases.

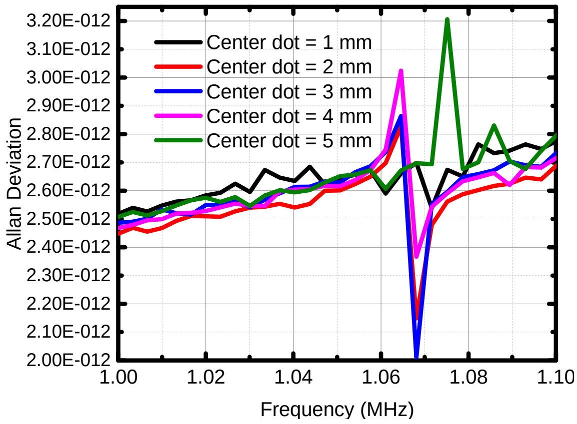

Fig. 3 (b). The curve which shows the calculated Allan deviation versus frequencies of five disks with different center dot electrodes.

4.2. Mass Sensitivity Coefficient and Detection Limit

The obtained σ (τ) as a function of frequencies was then used to calculate the detection limit; Δf (τ), as shown in Fig. 3(c). The disk with 3 mm as central diameter was found to be more sensitive and the maximum detection limit was approximately 2.15 μHz.

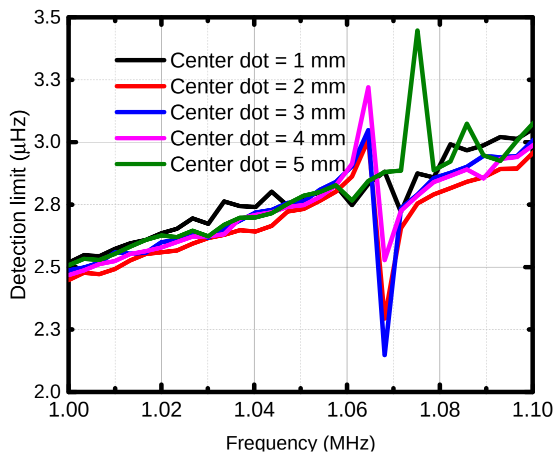

Fig. 3 (c). The curve which shows the calculated detection limit versus frequencies of five disks with different central diameters.

In Fig. 3 (d), are results showing the calculated mass sensitivity coefficients as a function of the measured frequencies, showing the specific mass sensitivity of approximately 2.6 $MHz.g^{-1}.cm^2$ when the resonant frequency is 1.07 MHz.

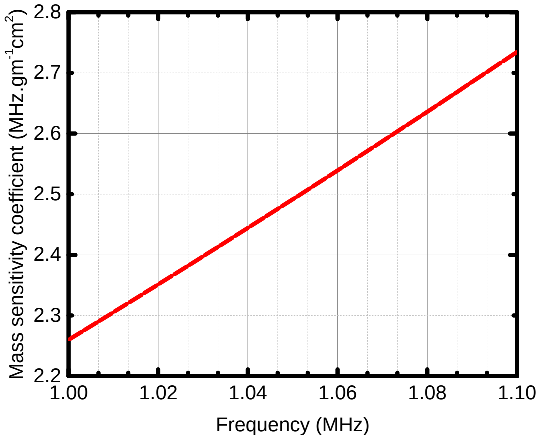

Fig. 3(d). The curve which shows the calculated mass sensitivity coefficients using Sauerbrey mass sensitivity coefficient equation.

4.3. Calculated Mass Resolution

The mass which can be detected on the surface of active center electrode area of each disk were calculated by taking the ratio of detection limit Δf (τ) in Fig. 3 (c) to mass sensitivity coefficient (K) in Fig. 3 (d). The curve which shows mass resolution per unit area of each disk is in Fig. 3 (e). The minimum mass resolution is 825 femtograms at 1.067 MHz for the disk with a diameter of 3 mm.

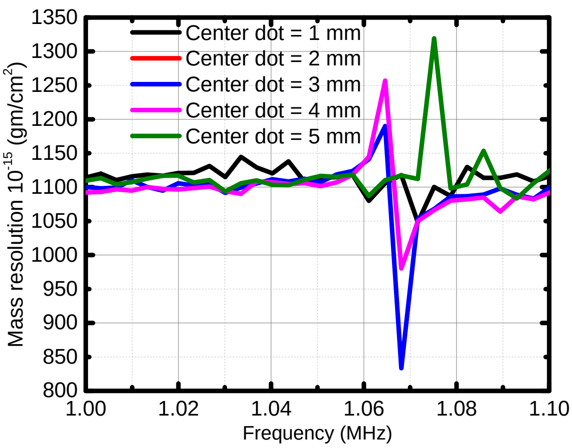

Fig. 3 (e). The curve which shows the calculated mass resolution as a function of frequencies and electrode diameters of five disks.

4.4. Measured Mass Using Frequency Shift

In order to convert the frequency shift to mass added on the surface of the active gold electrode, the Volume (V) of the Gold layer was calculated using the equation $\pi r^2 t$ where the thickness (t) is 3×10^{-5} cm and the radius (r) is 0.15 cm. The mass (m) of the Gold layer is calculated by multiplying the density of gold to the volume it occupies. Therefore the mass is given by multiplying $\pi r^2 t\times\rho$ = (3.14×0.15 cm × 0.15 cm × 3×10^{-5} cm) × (19.3 g/cm^3) = 4.09×10^{-5} g, where ρ is the density of Gold which is equal to 19.3 g/cm^3. The measured frequency shift (Δf) was 2×10^{-8} MHz when the resonant frequency (f) was 1.067 MHz. The frequency ratio (Δf/f) at resonance was found to be 1.9×10^{-8}. The mass change (Δm) is given by the expression: $\Delta f/f\times m = 1.9\times10^{-8}\times4.09\times10^{-5}$g = $=7.77\times10^{-13}$g. This mass is approximately 8.25×10^{-13} g/cm^2 calculated by taking the ratio of mass sensitivity coefficient to the detection limit, as seen in Fig. 3 (e). These results are almost the same as those reported by Mecea [23] with a frequency stability of $(\Delta f/f) = 1.5\times10^{-9}$, showing mass which is equivalent to 1 pg×cm^{-2}.

5. Challenges for Developing Diagnostic POC Based on QCM Mass Sensor

One of the challenges facing the development of femtogram mass sensors is particle selectivity and separation from the blood. Recently, biomarkers have shown good results for selectivity of certain virus, bacteria, cells, and molecules [24-28]. Moreover; the technological advances in microfluidic driven by ultrasonic acoustic forces which separate suspended particles in the fluid medium [29-32], have shown that it possible to combine QCM mass sensor technology with microfluidic to develop portable diagnostic POC. This review has shown that the separation technique based on microfluidic driven by ultrasonic acoustic forces is better than other conventional particle preparation and separation; using electro-spin [33], centrifuge [34], and BPS [35].

The conventional microfluidic techniques faces tremendous challenges such as:

1) Inconsistencies with diluting blood samples which causes inaccuracies into the measurements and reduced concentration of target analyses, leading to reduced assay sensitivity,

2) Complex designs that are cost-ineffective to integrate into microfluidic platforms,

3) Time consuming workflow systems with low extraction rates [36].

By using the new development of simplified microfluidic systems controlled with ultrasound standing waves, now it is possible to build a miniaturized microfluidic system for particles separation from whole blood [37-39]. This technology is currently used for separation of lipid particles in blood during major surgery, significantly reducing the embolic load to the brain after cardiac surgery [40]. Also, through this review, we noted that the low power ultrasonic acoustic forces can be used to separate suspended particles in the fluid in microscale to the nanoscale regime, while the high-power ultrasonic acoustic forces can be used to enhance industrial fluid/solid particle separation processes in macro scale [41].

6. Integration of Microfluidic to QCM Mass Sensor

In the flowchart shown in Fig. 4, the blood is injected into the microfluidic driven by ultrasonic acoustic forces which separate blood into cells, antigens, electrolytes, bacteria, and troponins. The components of the microfluidic delivery system are not discussed in this flowchart but include; micro pumps, micro valves, micro volumes, ultrasonic acoustic forces and a reflector, while the sensing components consist of biomarkers and special assay formats with gold nanoparticles on QCM. Successfully interfacing the microfluidic delivery system with QCM mass sensor will make it possible to develop cost-effective diagnostic POC system.

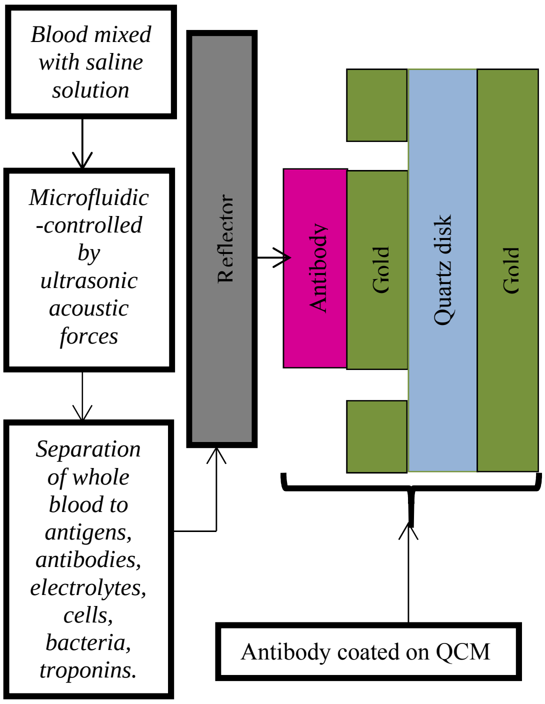

Fig. 4. The flow chart which shows blood flow into the microfluidic driven by ultrasonic acoustic standing wave attached to a sensor with antibody and gold, functionalized on QCM mass sensor.

7. Market Overview

The emerging market is expected to be in the home care, public health, agriculture, and food industry sectors. In the home care, there is a need to develop cost-effective diagnostic POC portable systems based on QCM mass sensor functionalized with anti-troponin [42-45]. Anti-troponin is gold standard sensitive biomarkers used to detect Myocardial Infraction (MI) by attracting troponin molecule from the blood. It is expected that troponin biomarkers could grow to encompass much of the diagnostic point of care (POC) market with a more sensitive and less expensive option [46]. The benefits of using POC tests can drastically increase patients' chances of survival as they can be administered much more quickly than lab tests in the hospitals [47]. A report [48] prepared by the Canadian Agency for Drugs and Technologies in Health (CADTH) estimated an annual cost of C$1,652,433,246 to do troponin (cTn) laboratory testing for suspected Acute Coronary Syndrome (ACS) patients, admitted through the emergency department in the hospital. This report showed that replacement of laboratory testing of cTn with POC devices could save billions of Canadian dollars and save the lives of many people by detecting the ACS before it happens in homes.

In the public health, agriculture and food industry sectors, the global cost to prevent and cure SARS outbreak was estimated to be 40 billion dollars [49] in 2003 while an outbreak of foot and mouth disease in the UK (2001) was about 5.8 billion dollars in reduced livestock production earnings [50]. Therefore, there is a need to use the existing inventions based on QCM mass sensor or any Bulk Acoustic Wave (BAW) biosensor which can detect a mass in femtogram regime, to build diagnostic POC equipment, for detecting SARS and foot and mouth diseases before infection. The global market for BAW biosensors was predicted to be 2000 to 17000 million US dollars from 2000 to 2018 and, valued to reach $22.68 billion [51] by 2020. Among these BAW biosensors, two-thirds is expected to be based on QCM mass sensor which is equivalent to $15.12 billion.

8. Conclusions

The QCM is limited to nanogram (10^{-9} g) but we have shown that it is possible to extend this technology to measure (10^{-13} g to 10^{-15} g) in the air. Also, we have shown that many inventions are reported to measure femtograms (10^{-15} g) but this technology does not exist due to the complexity of reproducing the claimed patents. Among these inventions, QCM disks are cost effective, currently available in the market, and can be reproduced easily. One of the future challenges is to integrate the sensor component with sample holders such as microfluidic, micro air, and microcentrifuge. The new development of novel ultrasonic acoustic standing wave devices for particle separation and nanoparticle/composite materials bioassays may provide suitable free-BPS POC solutions, which can overcome the matrix effects of whole blood.

The advances in bioassays have also led to increasing number of sensitive, smart and simplified POC based on whole blood, bypassing BPS, hence creating a rationale for its exclusion in use with "An Ultrasensitive High Q-factor QCM Mass Sensors" [52]. Also, we envision that a diagnostic POC with femtogram sensitivity will reduce the patient severity, death, false-positive hospital admittance, unnecessary costs to the hospital, and will have a potential to impact many scientific research fields; including medicine, nanotechnology, semiconductor manufacturing, and pharmaceutical research. This technology will create new business opportunities; therefore, creating new jobs in research institutions, hospitals, homeland security, pharmaceutical industries, and agriculture and food industry sectors.

Acknowledgments

I thank Prof. Thomas Thundat and Kenneth Cadien for their financial support, feedbacks, and for allowing me to use their laboratories. I also thank Dr. Prashanthi Kovur for helping me with Impedance measurements of my samples.

References

[1]. A. Sharma, E. Clark, J. D. McGlothlin, S. K. Mitta, Efficiency of airborne sample analysis platform (ASAP) bioaerosol sampler for pathogen detection, *Journal of Front. Microbiol.*, Vol. 6, 2015, pp. 1-7.

[2]. M. S. Petrovick, J. D. Harper, F. E. Nargi, E. D. Schwoebel, M. C. Hennessy, T. H. Rider, M. A. Hollis, Rapid sensors for biological-agent identification, *Lincolin Laboratory Journal*, Vol. 17, No. 1, 2007, pp. 63-84.

[3]. S. Faegh, N. Jalili, S. Sridhar, A self-sensing piezoelectric microcantilever biosensor for detection of ultra-small adsorbed masses: Theory and Experiments, *Sensors*, Vol. 13, No. 5, 2013, pp. 6089-6108.

[4]. M. L. Routes, K. L. Ekinci, Apparatus and method for ultrasensitive nanoelectromechanical mass detection, US Patent No. 6 722 200, 2004.

[5]. K. L. Ekinci, X. M. H. Huang, M. L. Roukesb, Ultrasensitive nanoelectromechanical mass detection, *Journal of Applied Physics Letters*, Vol. 84, No. 22, 2004, pp. 4469-4471.

[6]. N. V. Lavrik, P. G. Datskos, Femtogram mass detection using photo thermally actuated nanomechanical resonators, *Journal of Applied Physics*, Vol. 82, No. 16, 2003, pp. 2697-2699.

[7]. S. Dohn, W. Svendsen, A. Boisen, Mass and position determination of attached particles on cantilever based mass sensors, *Review of Scientific Instruments*, Vol. 78, No. 10, 2007, pp. 1033031-1033033.

[8]. M. Villarroya, *et al.*, System on chip mass sensor based on polysilicon cantilevers arrays for multiple detections, *Sensors and Actuators A: Physical,* Vol. 132, No. 1, 2006, pp. 154–164.

[9]. Y. T. Yang, C. Callegari, X. L. Feng, K. L. Ekinci, M. L. Routes, Zeptogram-scale nanomechanical mass sensing, *NANO Letters*, Vol. 6, No. 4, 2006, pp. 583-586.

[10]. B. Ilic, H. G. Craighead, S. Krylov, W. Senaratne, C. Ober, Atograms detection using nanoelectromechanical oscillators, *Journal of Applied Physics*, Vol. 95, No. 7, 2004, pp. 3694-3703.

[11]. S. Akita, T. Erie, Carbon nanotube mechanical resonators for mass sensing, *Sensors and Materials*, Vol. 21, No. 7, 2009, pp. 339-349.

[12]. Y. Dayagi, L. Dayan, M. Shalom, Sensitive and selective method and device for the detection of trace amounts of a substance, *US Patent* No. 7 159 463 B2, January 9, 2007.

[13]. V. Smith. R. Bhethanabotla, A. J. Richardson, Uniform mass sensitivity thickness shear mode quartz resonator, *US Patent* No. 8 215 171 B, July 2012.

[14]. W. Hin, Quartz crystal microbalance (QCM) mass sensor, Patent No. CN 102967521 B, April 2015.

[15]. C. K. O'Sullivan, G. G. Guilbault, Commercial quartz crystal microbalances – theory and applications, *Biosensors and Bioelectronics*, Vol. 14, No. 8-9, 1999, pp. 663–670.

[16]. R. E. Speight, M. A. Cooper, A survey of the 2010 quartz crystal microbalance literature, *Journal of Molecular Recognition*, Vol. 25, No. 9, 2012, pp. 451–473.

[17]. M. A. Cooper, V. T. Singleton, A survey of the 2001 to 2005 quartz crystal microbalance biosensor literature: applications of acoustic physics to the analysis of biomolecular interactions, *Journal of Molecular Recognition*, Vol. 20, No. 3, 2007, pp. 154–184.

[18]. B. Becker, M. A. Cooper, A survey of the 2006–2009 quartz crystal microbalance biosensor literature, *Journal of Molecular Recognition*, Vol. 24, No. 5, 2011, pp. 754–787.

[19]. M. Sauerbrey, Verwendung von schwingquarzen zur wägung dünner schichten und zur mikrowägung, *J. Zeitschrift Für Physik*, Vol. 155, No. 2, 1956, pp. 206-222.

[20]. G. O. Garcia-Martinez, *et al.*, Development of a mass sensitive quartz crystal microbalance (QCM)-based DNA biosensor using a 50 MHz electronic oscillator circuit, *Sensors*, Vol. 11, No. 8, 2011, pp. 7656-7664.

[21]. M. J. Moure, P. Rodiz, D. Valdes, L. F. Rodriguez-Padro, J. Farina, An FPGA-based system for the measurement of frequency noise and resolution of QCM sensors, *Latin American Applied Research*, Vol. 37, No. 1, 2007, pp. 25-30.

[22]. L. Rodriguez-Pardo, J. F. Rodriguez, C. Gabrielli, H. Perrot, Sensitivity, noise, and resolution in QCM sensors in liquid media, *IEEE Sensors Journal*, Vol. 5, No. 6, 2005, pp 1251-1257.

[23]. V. M. Mecea, Is quartz crystal microbalance really a mass sensor? *Sensors and Actuators A: Physical*, Vol. 128, No. 2, 2006, pp. 270–277.

[24]. S. P. Martin, R. J. Townsend, L. A. Kuznetsova, K. A. J. Borthwick, M. Hill, M. B. McDonnell, W. T. Coakley, Spore and micro-particle capture on an immunosensor surface in an ultrasound standing wave system, *Biosensors and Bioelectronics*, Vol. 21, No. 5, 2005, pp. 758-767.

[25]. O. Manneberg, B. Vanherberghen, J. Svennebring, H. M. Hertz, B. Onfelt, M. Wiklund, A three-dimensional ultrasonic cage for characterization of individual cells, *Journal of Applied Physics Letters*, Vol. 93, No. 6, 2008, p. 063901.

[26]. F. L. Dickert, P. Lieberzeit, O. Hayden, Sensor strategies for microorganism detection – from physical principles to imprinting procedures, *Analytical and Bioanalytical Chemistry*, Vol. 377, No. 3, 2003, pp. 540–549.

[27]. M. R. Gaso, C. M. Iborra, Á. M.Baides, A. A.Vives, Surface generated acoustic wave biosensors for the detection of pathogens: A Review, *Sensors*, Vol. 9, No. 12, 2009, pp. 5740-5769.

[28]. D. Klenerman, V. P. Ostanin, F. N. Dultsev, Measurement and use of molecular interactions, *United States Patent*, Patent No. US 6,589,727 B1, July 8, 2003.

[29]. F. Petersson, A. Nilsson, C. Holm, H. Jonssonc, T. Laurell, Separation of lipids from blood utilizing

ultrasonic standing waves in microfluidic channels, *Analyst*, Vol. 129, No. 10, 2004, pp. 938–943.

[30]. M. Gröschl, Ultrasonic separation of suspended particles - part I: fundamentals, *ACUSTICA- Acta Acustica*, Vol. 84, 1998, pp. 432-447.

[31]. N. Oyama, S. Yamaguchi, T. Shimomura, K. Miki, A method for detecting target sequences by oscillation frequency, *United States Patent*, Patent No. 5,552,274, Sep. 3, 1996.

[32]. J. J. Hawkes, W. T. Coakley, Force field particle filter, combining ultrasound standing waves and laminar flow, *Sensors and Actuators B: Chemical*, Vol. 75, 2001, pp. 213-222.

[33]. Y. S. Park, V. Sunkara, Y. Kim, W. S. Lee, J. R. Han, Y. K. Cho, Fully automated centrifugal microfluidic device for ultrasensitive protein detection from whole blood, *Journal of Visualized Experiments*, Issue 110, 2016, pp. 1-7.

[34]. D. R. Gossett, W. M. Weaver, A. J. Mach, S. C. Hur, H. T. Tse, W. Lee, H. Amini, D. D. Carlo, Label-free cell separation and sorting in microfluidic systems, *Analytical* and *Bioanalytical Chemistry*, Vol. 397, No. 8, 2010, pp. 3249-3267.

[35]. S. Tripathi, Y. V. Bala, V. Kumar, A. Prabhakar, S. S. Joshi, A. Agrawal, Passive blood plasma separation at the microscale: a review of design principles and microdevices, *Journal of Micromechanics and Microengineering*, Vol. 25, No. 8, 2015, pp. 1-24.

[36]. W. S. Mielczarek, E. A. Obaje, T. T. Bachman, M. Kersaudy-Kerhoas, Microfluidic blood plasma separation for medical diagnostics: is it worth it?, *Lab on a Chip*, Vol. 16, No. 18, 2016, pp. 3441-3448.

[37]. D. G. Sadikova, T. N. Pashovkin, Cell concentration and separation in the field of a standing ultrasonic wave for medicine and biotechnology, *Open Journal of Biophysics*, Vol. 3, No. 1A, 2013, pp. 70-75.

[38]. A. Włoch, H. Czy, T. Jasiski, Ultrasonic methods of the cells separation in human blood, *Acta Physica Polonica A*, Vol. 128, No. 2, 2015, pp. 234-236.

[39]. H. Jonsson, A. Nilsson, F. Petersson, M. Allers, T. Laurell, Particle separation using ultrasound can be used with human shed mediastinal blood, *Perfusion*, Vol. 20, No. 1, 2005, pp. 39-43.

[40]. D. Bergman, I. M. Hartvig, S. Uhrberg, Assay device and method, WO 2005089082 A2, Application No. PCT/SE2005/000429, Sep 29, 2005.

[41]. E. R. Sarabia, J. A. Gallego-Juarez, G. R. Corral, L. E. Segura, Application of high-power ultrasound to enhance fluid/solid particle separation processes, *Ultrasonic*, Vol. 38, No. 1-8, 2000, pp. 642–646.

[42]. T. Keller, *et al*., Sensitive troponin I assay in early diagnosis of acute myocardial infarction, *The New England Journal of Medicine (NEJM)*, Vol. 361, No. 9, 2009, pp. 868-877.

[43]. D. B. Diercks, *et al*., Diagnostic accuracy of a point-of-care troponin I assay for acute myocardial infarction within 3 hours after presentation in early presenters to the emergency department with chest pain, *American Heart Journal*, Vol. 163, No. 1, 2012, pp. 74-80.

[44]. T. Reichlin, *et al.,* One-hour rule-out and rule-in of acute myocardial infarction using high-sensitivity cardiac troponin T, *Arch. Intern. Med*, Vol. 172, No. 16, 2012, pp. 1211-1218.

[45]. B. Cummins, *et al*., Cardiac-specific troponin-I radioimmunoassay in the diagnosis of acute myocardial infarction, *American Heart Journal*, Vol. 113, No. 6, 1987, pp. 1333-1344.

[46]. P. B. Luppa, Carolin Muller, Alice Schlichtiger, Harald Schlebusch, Point-of-care testing (POCT): Current techniques and future perspectives, *Trends* in *Analytical Chemistry*, Vol. 30, No. 6, 2011, pp. 887-898.

[47]. P. von Lode, Point-of-care immune testing: Approaching the analytical performance of central laboratory methods, *Clinical Biochemistry*, Vol. 38, Issue 7, 2005, pp. 591-606.

[48]. Canadian Agency for Drugs and Technologies in Health (CADTH), Point-of-care cardiac troponin testing in patients with symptoms suggestive of acute coronary syndrome, *CADTH Optimal Use Report*, No. 5.1a, 2015, pp. 1-3.

[49]. J. W. Lee, W. J. McKibbin, Estimating the global economic costs of SARS, website at http://www.ncbi.nlm.nih.gov/books/NBK92473/

[50]. D. L. P. J. Leatherman, T. C. Schroeder, G. S. Alward, The economic impact of foot –and- mouth disease outbreak region analysis, website at http://ageconsearch.umn.edu/bitstream/10252/1/sp07pe01.pdf

[51]. Biosensors Market worth $22.68 Billion by 2020, website at http://www.marketsandmarkets.com/Market-Reports/biosensors-market-798.html

[52]. S. Seif, T. Thundat, K. Cadien, An Ultrasensitive AT-Cut quartz crystal microbalance femtogram mass sensor, US-Provision Patent No. 2016010-072-82-25, filled November 2016.

___

Published by International Frequency Sensor Association (IFSA) Publishing, S. L., 2017 (http://www.sensorsportal.com).